



HAL
open science

Incidence angle effect: results of an interlaboratory comparison of measurements on commercial-size modules

Mauro Pravettoni, Min Hsian Saw, Giorgio Bardizza, Giovanni Bellanda, Romain Couderc, Gabi Friesen, Werner Hermann, Shin Woei Leow, Stefan Riechelmann, Flavio Valoti, et al.

► To cite this version:

Mauro Pravettoni, Min Hsian Saw, Giorgio Bardizza, Giovanni Bellanda, Romain Couderc, et al.. Incidence angle effect: results of an interlaboratory comparison of measurements on commercial-size modules. Progress in Photovoltaics, 2024, pp.1-11, 2024, Progress in Photovoltaics, 10.1002/pip.3850 . cea-04720673

HAL Id: cea-04720673

<https://cea.hal.science/cea-04720673v1>

Submitted on 3 Oct 2024

HAL is a multi-disciplinary open access archive for the deposit and dissemination of scientific research documents, whether they are published or not. The documents may come from teaching and research institutions in France or abroad, or from public or private research centers.

L'archive ouverte pluridisciplinaire **HAL**, est destinée au dépôt et à la diffusion de documents scientifiques de niveau recherche, publiés ou non, émanant des établissements d'enseignement et de recherche français ou étrangers, des laboratoires publics ou privés.

INCIDENCE ANGLE EFFECT: VALIDATION OF NEW MEASUREMENT METHODS FOR IEC 61853-2

Mauro Pravettoni¹, Min Hsian Saw^{1,2}, Giorgio Bardizza³, Giovanni Bellenda⁴, Romain Couderc⁵, Gabi Friesen⁴, Werner Herrmann³, Shin Woei Leow², Stefan Riechelmann⁶, Flavio Valoti⁴, Arvid van der Heide⁷, Frank Weinrich⁶ and Stefan Winter⁶

¹ Technology Innovation Institute (TII), Renewable and Sustainable Energy Research Center, Abu Dhabi, UAE

² National University of Singapore, Solar Energy Research Institute of Singapore (SERIS), Singapore

³ TÜV-Rheinland, Cologne, Germany

⁴ Scuola Universitaria Professionale della Svizzera Italiana (SUPSI), Istituto di Sostenibilità Ambientale Applicata all'Ambiente Costruito (ISAAC), Mendrisio, Switzerland

⁵ CEA, Institut National de l'Energie Solaire (INES), Le Bourget-du-lac, France

⁶ Physikalisch-Technische Bundesanstalt (PTB), Braunschweig, Germany

⁷ IMEC, IMO-IMOMEC / Energyville, Genk, Belgium

ABSTRACT: The incidence angle effect causes a decrease in the photogenerated current of PV modules when they are subject to incident irradiance at wide angles: its relevance should be quantified for accurate energy yield purposes and has recently gained significance due to the rising interest in innovative vertically integrated PV applications (e.g. in urban structures, in agrivoltaics, and vehicles). The international standard IEC 61853-2 presents both an outdoor and an indoor measurement method: however, the indoor measurement method for commercial-size modules is often impractical due to irradiance uniformity limitations on the volume spanned by the tested module upon rotation in most of the solar simulators available on the market. In recent years, new solutions have been proposed to overcome these limitations and allow wider adoption of this standard: however, method validations and interlaboratory comparisons have been conducted so far only at small-area samples and a real validation on commercial-size modules is still missing. In this work we aim at filling this gap, reporting the results of an interlaboratory comparison conducted within the international Project Team that is currently working at the new edition of IEC 61853-2. The results show a remarkable agreement between different measurement methods, thus validating more options for the evaluation of this important effect.

Keywords: Antiglare Treatment, Energy Rating, Experimental Methods, Incidence Angle Modifier, Relative Angular Transmittance

1 INTRODUCTION

By incidence angle effect we mean the decrease in the photogenerated current of photovoltaic (PV) modules when they are subject to direct incident irradiance at wide angles. The relative light transmittance through the transparent encapsulants into the module is primarily influenced by the reflectivity of the first glass-to-air interface: anti-glare treatment may be applied to reduce reflections and enhance light transmittance at wide angles. The relevance of this effect may be quantified for energy rating purposes. It is also needed for an accurate energy yield prediction, which, among other thermal and radiative effects, should take also into account the incidence angle effect when the direct solar irradiance reaches the solar modules at wide angles. Therefore, it has recently gained significance due to the rising interest in novel integrated PV applications, where vertical or non-optimal tilt are favoured (e.g. in agrivoltaics, integration into vehicles, buildings, etc.), or where antiglare is of interest (e.g. in buildings, urban infrastructures, airport installations, etc.).

Among the International Electrotechnical Commission (IEC) standards, measurement methods for the incidence angle effect are described in the IEC 61853 energy rating series. Its Part 2 (in Ed. 1.0 at the time of writing [1]) describes two procedures: an indoor method, requiring a solar simulator with minimum Class B spatial uniformity of irradiance upon full rotation of the test device (i.e. $\pm 5\%$, according to IEC 60904-9 [2]); and an outdoor method, requiring a two-axis tracker to provide rotation of the test device with respect to normal incidence and means of subtracting the diffused component of irradiance from the direct one. In both cases, the measured quantity is the relative internal angular transmittance $\tau_{rel}(\theta)$, which is also commonly referred to as incidence angle modifier (IAM) and can be interpolated with the following analytical function [3-4]

$$\tau_{rel}(\theta) = \frac{1 - e^{-\frac{\cos \theta}{a_r}}}{1 - e^{-\frac{1}{a_r}}} \quad (1)$$

where θ is the angle of incidence and a_r is a dimensionless interpolation parameter.

The indoor method of IEC 61853-2 was proven over the years to be particularly problematic: the minimum Class B uniformity requirement in it, far from being sufficient to provide accurate measurements,

is still challenging to meet, even with commercially available solar simulators with Class A+ uniformity. The standard allows for testing smaller-size, optically equivalent modules, for which the Class B uniformity requirement should be more easily reached. Another option allowed by the standard is to isolate electrically one cell in the test module so that the active module area can span a limited volume fulfilling the uniformity requirements: this can be done destructively by cutting the backsheet and by connecting directly the busbars at the terminals of the target cell.

W. Herrmann et al. [5] proposed an innovative method to overcome the spatial uniformity limitations on full-size modules: the method is non-destructive, it can measure PV modules of any size and is based on inferring the short-circuit current contribution of a partially shaded cell in the module under test from a set of current-voltage measurements at different angles. The partial-shading method allows to limit the Class B requirement of IEC 61853-2 to the volume of rotation of the single target cell, notwithstanding the real dimensions of the test module.

Recognizing the importance of stray light and its potentially relevant impact on measurement accuracy, the method was later improved [6] by introducing a straightforward procedure to subtract the unintended irradiance that may be diffused by the laboratory walls to the test module or reflected by it and then diffused back by the laboratory environment. Meanwhile, other methods appeared in the literature (a comprehensive review of them can be found in [7]). Amdemeskel et al. [8] proposed an under-irradiation method (i.e. a method where the light source only partially covers the target cell), where a spot-area laser beam is projected on a test plane where the test cell is rotated along its axis. Saw et al. [9] used a similar approach with a Xenon light source delivered to the target via an optical fibre and an angular probe holder, where a collimator at the output of the fibre is slotted at different angles of incidence. The method was validated versus the indoor method of IEC 61853-2 on single-cell minimodules and the same approach was later upgraded to the module level by Pravettoni et al. [10]. Plag et al. [11] introduced a spectrally selective method, based on angular-dependent measurements of spectral responsivity.

The outdoor test method of IEC 61853-2 has also been the object of various adjustments in the literature. King et al. [12] presented the results of their outdoor method enabling modules to be tested over the full range of 0-90 ° by articulating the tracker in elevation only and using a shaded pyranometer to make a direct measurement of the diffuse component, thus reducing significantly measurement uncertainty. Coston et al. [13] observed an up to 4% non-uniformity of irradiance reaching the cells across the surface of a 72-cell test module: the authors suggested that this effect is the result of a combination of light trapping within the top sheet glass layer and reflections from the aluminum frame at the edge of the module. Riechelmann et al. [14] presented their outdoor measurement apparatus (a rectangular black tube with a volume of $4 \times 4 \times 7.2$ m³, capable of tracking the sun and blocking most of the diffuse component of irradiance), in which a module holder inside the tube can be tilted relative to the sun, enabling to perform accurate measurements of the angle of incidence effect as close as possible to the ideal conditions (i.e. AM1.5, collimated and uniform 1000 W/m² total irradiance). One last approach was provided by van der Heide et al. [15], which is based on the simultaneous measurement of the test sample and a reference module, both placed co-planarly on a 2-axis tracker: the reference module shall have a calibrated relative internal angular transmittance and allow quick measurement of the incidence angle effect of the test sample via rotating both testing and reference modules away from the direct solar beam and varying the angle of incidence from 0 ° to 90 °.

This variety of modified or new methods suggested the IEC Technical Committee 82 to finally revise IEC 61853-2 and prepare a new edition 2.0 including any new method that proved to be reproducible, thus widening the options for testing laboratories and module manufacturers and facilitating a wider adoption of the standard itself. The Committee Draft (CD) that is currently in preparation proposes 6 possible methods for the measurement of the incidence angle effect, as follows:

- Indoor method 1 (“irradiation of a full cell or module or optically equivalent device”), which is equivalent to the indoor method of Ed. 1.0 [1];
- Indoor method 2 (“irradiation of a partially shaded cell in a module”), based on the method described in [5];
- Indoor method 3 (“partial irradiation”), based on the method described in [8-9] (for cells) and [10] (for modules);
- Indoor method 4 (“spectrally resolved method”), based on the method described in [11];
- Outdoor method 1 (“absolute method”), which is equivalent to the outdoor method of Ed. 1.0 [1], with amendments following the cited works [12-14];
- Outdoor method 2 (“relative method”), based on the method described in [15].

The objective of this work is to demonstrate the reproducibility of the new methods with reference to the outdoor method 1, hence to validate them for inclusion in the CD version of edition 2.0 of IEC 61853-2.

This is achieved via an interlaboratory comparison that, rephrasing ISO/IEC 17043 [16], has precisely the purpose of establishing "the effectiveness of measurement or test methods and the comparability of measurement or test results". "Identification of differences in measurement or test results" and "validation of measurement uncertainty claims" are other important findings in interlaboratory comparisons and help the participant laboratories to adopt one of the proposed testing methods with proof of competency.




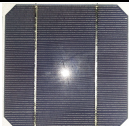

The structure of the article is as follows: section 2 illustrates the scheme adopted for the interlaboratory comparison, with a description of the test samples, participant laboratories, and statistical approach adopted for performance evaluation; section 3 shows and describes the measurement results, while section 4 discusses the observed differences and shows the reproducibility of the proposed methods; the conclusions are in section 5.

2 THE INTERLABORATORY COMPARISON SCHEME

2.1 Test samples

Table 1 shows the three test samples that were distributed to the participants of the interlaboratory comparison. These were provided by the Solar Energy Research Institute of Singapore (SERIS) and are: a 72-cell silicon heterojunction (HJT) module by Sanyo, a 120-half-cut-cell polycrystalline silicon (poly-Si) module by REC and a 60-cell poly-Si module by Gintung. All modules were commercially available at the time of production and are a representative selection of a variety of products in the field: in fact, although no longer mainstream, poly-Si is still vastly deployed; HJT, pioneered by Sanyo with the proposed sample, is foreseen to become mainstream in the next years, due to its promising efficiency. Finally, the Gintung sample has a peculiar antiglare treatment, which can be visually observed when a spot of light is shone on top of it, as illustrated in the last row of Table 1: this module was specifically selected to include a sample with expected different angular transmittance properties.

Table 1 – Test samples:

			
Manufacturer:	Sanyo (HIP series)	REC (TwinPeak 2 series)	Gintung (WG series)
Model:	HIP-215NKHE5	REC275TP2	WG-280P6A
Cell technology:	c-Si (HJT)	poly-Si	poly-Si
Cell configuration:	72 cells, full size	120 cells, half-cut	60 cells, full size
Dimensions [mm ²]:	1580 × 798	1675 × 997	1640 × 992
<i>I</i> _{sc} [A]:	5.61	9.52	9.40
Antiglare treatment:	No	No	Yes
Effect of glare:			

2.2 Measurement methods and participants

The six participant laboratories in the interlaboratory comparison were: SERIS Testing Laboratory of the National University of Singapore (which coordinated the exercise with the support of TII, a research institute in Abu Dhabi), TÜV-Rheinland in Cologne (Germany), SUPSI PV Lab in Mendrisio (Switzerland), the Institut National de l'Énergie Solaire (INES) of CEA in Le Bourget-du-lac (France), the Physikalisch-Technische Bundesanstalt (PTB) in Braunschweig (Germany) and EnergyVille laboratory at IMEC in Genk (Belgium). SERIS, TÜV-Rheinland, SUPSI, and INES are ISO/IEC 17025 accredited laboratories for the electrical testing of PV modules, TÜV-Rheinland being also a renowned certification body in the field; PTB,

the German national metrology institute, is ISO/IEC 17025 accredited for PV calibrations; EnergyVille has renowned experience in outdoor PV measurements.

Table 2 lists the six methods of the CD of IEC 61853-2 (Ed. 2.0) circulating at the time of writing. The participant laboratories were randomly labelled from Lab 1 to Lab 6 (where the numbering does not correspond to the sequential order of measurements) and have adopted the indoor methods 2 (Lab 2, 4 and 5) and 3 (Lab 3), and the outdoor methods 1 (Lab 6) and 2 (Lab 1). The indoor methods 1 and 4 were not tested during the interlaboratory comparison.

Table 2 – Measurement methods according to the current Ed. 1.0 of IEC 61853-2 and the four additional new methods proposed in the circulating CD for its Ed. 2.0, with the anonymous identification of the participating laboratories:

Measurement method	IEC 61853-2		Random identification
	Ed 1.0	Ed 2.0 (CD)	
Indoor method 1 (full irradiation)	Yes	Yes	-
Indoor method 2 (full irradiation on a partially shaded cell)	No	Yes	Lab 2*
			Lab 4
			Lab 5
Indoor method 3 (partial irradiation with lock-in)	No	Yes	Lab 3
Indoor method 4 (spectrally selective)	No	Yes	-
Outdoor method 1 (absolute method)	Yes	Yes	Lab 6
Outdoor method 2 (relative method)	No	Yes	Lab 1

*Lab 2 used a procedure for the subtraction of straylight, which was not adopted by Lab 4 and 5.

2.3 Method validation and statistical design

To validate the four new measurement methods of Table 2, the three samples of Table 1 were circulated in a sequential scheme (commonly referred to as “round-robin”), in which all participant laboratories measured all the samples in the following sequence: SERIS, TÜV-Rheinland, SUPSI, INES, PTB and EnergyVille. Since in the round-robin scheme all participants measure all modules, there is no homogeneity requirement for the test samples.

The assigned values (i.e. the “true” values attributed to the relative angular transmittance as a function of the incidence angle and to the interpolation parameter a_r) were determined by *consensus* as the median (a well-known outlier-resistant estimator of the population mean [17]) of the non-outlying measurement results after all participants have completed their measurement (the procedure for outlier removal is described in section 2.4). The results of participant laboratories are compared considering their claimed measurement uncertainties via assignment of E_n scores, defined as [17]

$$E_n = \frac{x_i - x_{ref}}{\sqrt{U_i^2 + U_{ref}^2}}, \quad (2)$$

where x_i and x_{ref} are the i -th laboratory’s measurement and assigned value, respectively; U_i and U_{ref} are the expanded uncertainties (confidence level of approximately 95%) of the i -th laboratory and the assigned value, respectively. U_{ref} was calculated by doubling the following *scaled median absolute deviation* (MADe, an estimate of the population standard deviation that is highly resistant to outliers [17])

$$MADe(x_i) = 1.483 \cdot med(d_i), \quad (3)$$

where $med(d_i)$ is the median of the absolute deviations $d_i = |x_i - x_{ref}|$.

The stability of the relative angular transmittance properties of the test samples was reasonably assumed, hence the exercise ended when the last participant laboratory completed its measurements. To ensure modules were not subject to risks of mechanical shocks and microcracks that may affect their relative transmittance properties, the samples were shipped in an Air Transport Association (ATA) standard case and laboratories were asked to verify their integrity with electroluminescence imaging.

2.4 Outlier removal, assigned values and their uncertainty

The following procedure was applied for outlier removal:

- **First scoring:** Assigned values, their uncertainty and E_n scores are calculated for all participants as described in section 2.3;
- **First round of outlier removal:** Any participant scoring $|E_n| > 1$ is considered an outlier and removed;
- **Second scoring:** Assigned values, their uncertainty and E_n scores are then recalculated for the restricted pool of non-outlying participants after the first round of outlier removal;
- **Second round of outlier removal:** Any participant scoring $|E_n| > 1$ is considered an outlier and removed;
- **Convergence or divergence:** The procedure of the previous points is repeated with further rounds

of scoring and outlying removals until a minimum of three participant laboratories score $|E_n| < 1$ for all measurands: when this occurs (*convergence*), the assigned values and their uncertainties are set; in case this does not occur (*divergence*), the reproducibility of measurements is considered poor, and no assigned value is set.

If convergence occurs, two scenarios are possible. In the first scenario, the three converging laboratories are all using the same test method of Table 2: in this case (that in our interlaboratory comparison was possible only for the indoor method 2) that method is reproducible, but the reproducibility between all methods fails. In the second scenario, the converging laboratories use different test methods in Table 2: in this case, the reproducibility between these methods is successful.

3 RESULTS AND UNCERTAINTIES

3.1 Relative angular transmittance measurements

The reported EL imaging showed no evidence of damage to the modules during the exercise. Figure 1 shows the results of the measured relative angular transmittance $\tau_{rel}(\theta)$ as a function of the angle of incidence θ by the six participant laboratories and for the three test samples of Table 1: Sanyo (Figure 1a), REC (Figure 1b) and Gintung (Figure 1c). The charts highlight in red the outlying measurements and in continuous black lines the assigned values. All measurements were performed with axis of rotation parallel to the busbars. All laboratories measured at θ ranging at least from -80° to 80° , step 10° .

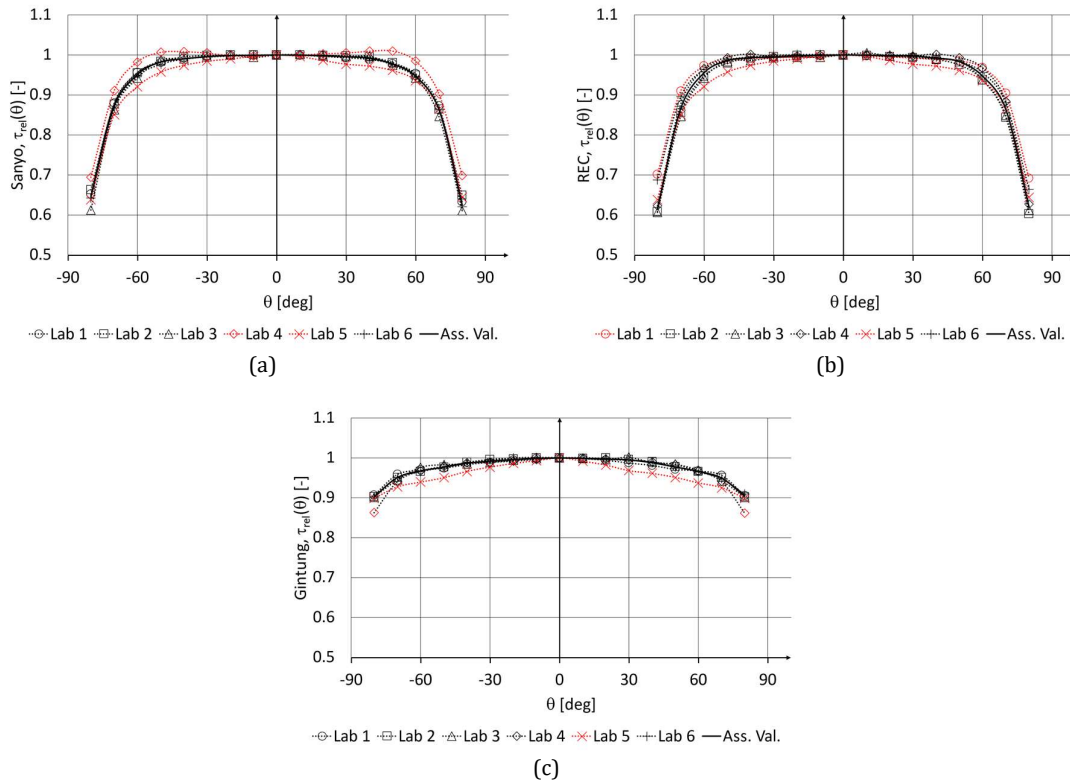


Figure 1: Relative angular transmittance, measurement results: (a) Sanyo; (b) REC; and (c) Gintung. Red data indicate outlying measurements; the continuous line indicates the assigned value (see section 2.3). All measurements were performed with axis of rotation parallel to the busbars.

Figure 1a (the Sanyo sample) shows that Lab 4 and 5 were outlying, while Lab 1, 2, 3 and 6 showed reproducible measurement results. Lab 4 showed 3-5% higher relative angular transmittance at $|\theta| > 30^\circ$. The outliers of Lab 5 indicate lower relative angular transmittance at $20^\circ < |\theta| < 60^\circ$.

Figure 1b (REC) shows slightly different findings: here Lab 2, 3, 4 and 6 showed reproducible measurement results with slightly higher relative angular transmittance reported by Lab 6 at wide negative incidence angles, which is tight to measurement uncertainty and indicates a minor asymmetry in $\tau_{rel}(\theta)$ that was not confirmed by Lab 2, 3 and 4, but similarly to the slightly outlying results of Lab 1. Lab 5 was still outlying, showing the same trends already observed for the Sanyo sample. Overall, the spread of

measurements of the REC samples between non-outlying laboratories is larger than with Sanyo and Gintung samples, contributing to larger uncertainties in the assigned values.

On the contrary, Figure 1c (Gintung) shows the best reproducibility between all laboratories except for Lab 5 and the measurements at $\pm 80^\circ$ from Lab 4 only.

3.2 Interpolation parameter a_r

Figure 2 shows the comparison between the interpolation parameters a_r for the three samples of Table 1, as reported by the 6 participants. The black columns indicate the assigned values, calculated as the median of the values reported by the non-outlying laboratories in relative angular transmittance measurements. The error bars indicate the expanded uncertainty of the reported and assigned values (coverage factor $k = 2$, corresponding to approximately 95% confidence level). The a_r values showed few outlying cases, i.e. Lab 4 and 5 with the Sanyo sample only: this is partly due to the high level of reproducibility for that sample within the non-outlying laboratories (Lab 1, 2, 3 and 6), resulting in a lower uncertainty in the assigned value.

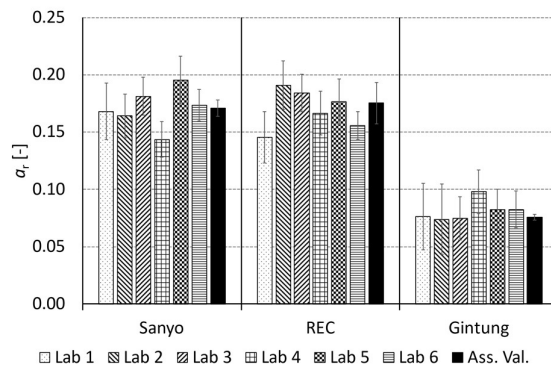


Figure 2: Calculated interpolation parameters a_r for the relative angular transmittance measurements of Figure 1, as defined in IEC 61853-2. The black columns indicate the assigned values (see section 2.3). The error bars indicate expanded uncertainty (coverage factor $k = 2$, corresponding to a confidence level of approximately 95%).

3.3 Uncertainty considerations

Indoor test methods 1 and 2 are typically performed in “tunnel” solar simulators (i.e. solar simulators where the distance between the light source and the target is several metres and the source can be considered in good approximation as point-like). With this apparatus, the dominant uncertainty contributions are irradiance non-uniformity, stray light and angular positioning. The spatial uniformity requirement set in IEC 61853-2 for solar simulators is minimum Class B (i.e. $\pm 5\%$ [2]) over the volume of rotation of the active area: Lab 2, 4 and 5 used a simulator with Class A+ uniformity, for which the contribution to the uncertainty increases up to $\sim 1\%$ (with rectangular distribution) at $\pm 80^\circ$. Probably the most important uncertainty contribution with indoor method 1 and 2 is the effect of stray light: this can be due to the irradiance diffused by the walls of the darkroom, or irradiance reflected by the test sample to the walls and then diffused back to the sample (secondary reflections). This stray light effect can be mitigated using the subtraction procedure used by Lab 2 and presented in [6]. Angular positioning is another important uncertainty at the widest angles, due to the cosine effect: an uncertainty of $\pm 0.5^\circ$ in positioning can contribute with up to $\pm 2.5\%$ uncertainty at $\theta = 80^\circ$. Overall, a typical uncertainty with indoor test methods 1 and 2 can be as high as $\pm 5\%$ at $\theta = 80^\circ$ ($k = 2$, approximately 95% confidence).

The degree of accuracy of the incidence angle of the collimated beam, spectral match of the light source to AM1.5 and uncertainty in data acquisition with the lock-in technique are the dominant uncertainty contributions in the indoor test method 3. A significant measurement bias can come from the interference between the incident beam and the busbars when the axis of rotation is parallel to them: this should be accurately avoided as detailed in [9] for accurate measurements and reproducible results. Typical uncertainty with indoor test methods 3 can also be as high as $\pm 5\%$ at $\theta = 80^\circ$ [10].

The outdoor method 1 approaches in principle the most ideal measurement conditions, with perfect spatial uniformity, incident light collimation and negligible spectral match. Angular positioning (particularly at wide angles) and the effect of stray light by the surrounding environment are usually the dominant uncertainty contributions in this method: if mitigated or corrected accurately, the uncertainty can

be kept within ± 2 or $\pm 3\%$ at angles of incidence as high as 70° ; but, the same as in the indoor methods, the uncertainty of $\pm 0.5^\circ$ in positioning can raise the overall uncertainty budget to up to $\pm 4\%$ or more at $\theta = 80^\circ$. The outdoor method 2 has various practical advantages, but it carries the uncertainty in the calibration of the relative angular transmittance of the reference device, which can easily contribute to rising the overall uncertainty above 6% at wide angles (the other dominant contributions being alignment, positioning and stray light).

Equation (1) that defines the interpolation parameter a_r does not allow a straightforward analytical method to evaluate the uncertainty in this parameter from the uncertainties in the measured relative angular transmittance $\tau_{rel}(\theta)$ and in the incidence angle θ . Therefore, in this work we first defined a_r^+ and a_r^- as the interpolation parameters of the limit superior and inferior $\tau_{rel}^+(\theta) = \tau_{rel}(\theta)(1 + U)$ and $\tau_{rel}^-(\theta) = \tau_{rel}(\theta)(1 - U)$, respectively; then we assumed the uncertainty in a_r to be triangularly distributed (coverage factor $k = \sqrt{6}$) around a_r in a range equal to the largest of the possible deviations $|a_r - a_r^\pm|$.

The expanded uncertainty in the assigned value x_i ($k = 2$, approximately 95% confidence) was taken doubling the scaled median absolute deviation $MADe(x_i)$, which, as discussed in section 2.3 is a robust estimate of the population standard deviation. As is often the case in interlaboratory comparison, the uncertainty in the assigned values is higher when the level of reproducibility of the non-outlying laboratories is lower.

4 DISCUSSION

4.1 E_n scores

Figure 3 shows the comparison between the E_n scores of all laboratories in all measurements as follows: for the relative angular transmittance of the Sanyo sample (Figure 3a), of the REC sample (Figure 3b), of the Gintung sample (Figure 3c), and for the interpolation parameter a_r (Figure 3d). Measurements with $|E_n| > 1$ are marked in red: these indicate cases where the measurement procedure caused a bias between the measured and the assigned values, which is not expected by the reported measurement uncertainty. In proficiency testing practice, these cases should lead to further verification of the measurement procedure or a revision of the uncertainty evaluation.

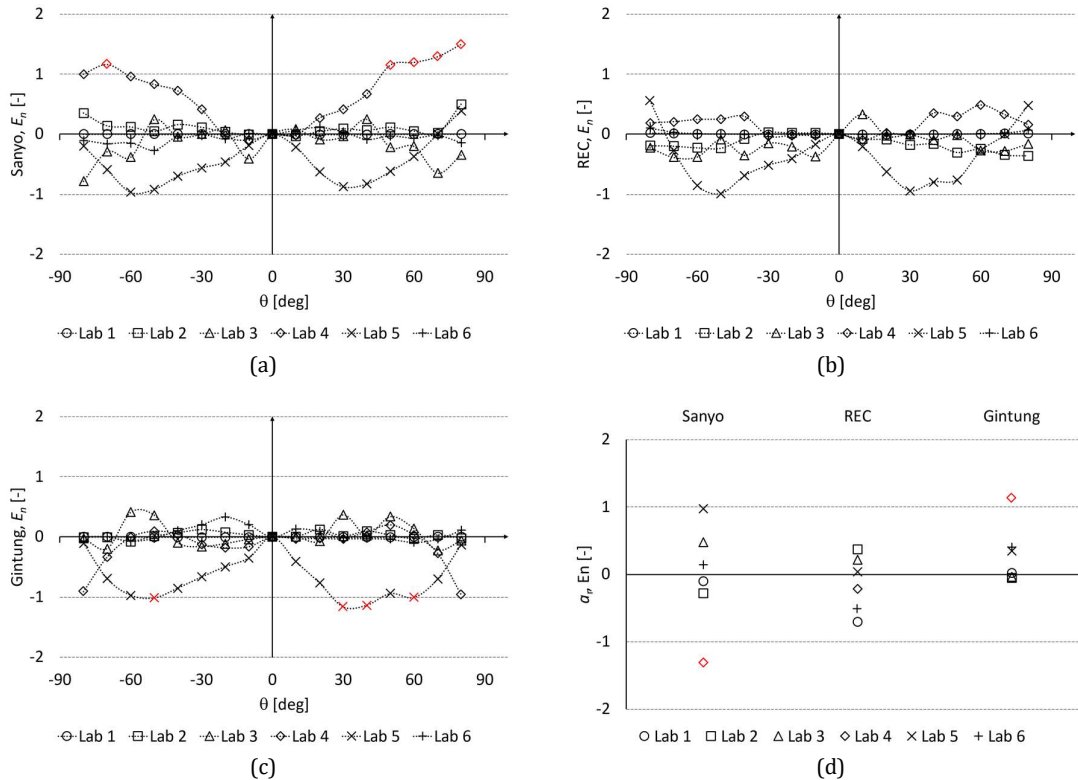


Figure 3: E_n scores for: (a) Sanyo; (b) REC; (c) Gintung; and (d) a_r values. Scores $|E_n| > 1$ (in red) indicates an unsuccessful measurement performance and should lead to a review in the uncertainty estimate or to a correction of a measurement issue: this is the case of Lab 4 on Sanyo and Gintung, while Lab 5 value is borderline on Sanyo.

Figure 3a confirms the observations of Figure 1a that Lab 4 is outlying, measuring higher relative angular transmittance on the Sanyo module than Lab 1, 2, 3 and 6. Lab 5, instead, which has outlying results as well in Figure 1a with lower relative angular transmittance measurements, scores $-1 < E_n < 0$, indicating that the observed deviations from the assigned values are still consistent with measurement uncertainty.

The higher uncertainty in the assigned values of the REC module (Figure 3b) resulted in the overall performance of all laboratories with $|E_n| \lesssim 1$ scores, with questionable measurements of Lab 5 between 30° and 60° in both directions.

The Gintung sample (Figure 3c) is where the degree of reproducibility is the highest, with all labs showing very good performance ($|E_n| < 0.5$), except for Lab 5 and questionable E_n scores only at $\pm 80^\circ$ from Lab 4. This is significant since this sample has a very peculiar antiglare treatment that ultimately did not represent an additional challenge for the participants.

Calculation of the interpolation parameter a_r also showed a high level of reproducibility for the REC and Gintung samples, which is good news for the work towards the revision of IEC 61853-2: however, this result is partially caused by the high uncertainty (order of 10%) with which this parameter is calculated and that should be improved. Lab 4 showed an outlying performance on Sanyo (for which also Lab 5 is borderline) and Gintung: this is consistent with the deviations observed in the measurements of relative angular transmittance.

4.2 The reproducibility between Lab 1, 2, 3 and 6

Lab 2, 3 and 6 remarkably obtained reproducible results using the four different measurement methods (indoor method 2 and 3 and outdoor method 1): the median of their results contributed to determining the assigned values for all test samples (with the inclusion of Lab 4 for the Gintung sample). Lab 1 (using outdoor method 2) showed results that were slightly outlying in the REC case and were therefore removed for the calculation of the assigned values of that sample: however, within its measurement uncertainty, the results of Lab 1 showed $|E_n| < 1$ with all samples.

Since outdoor method 1 is the method where the measurement conditions are the closest to the ideal conditions of irradiance (1000 W/m² total irradiance, AM1.5 spectral irradiance, and collimated direct irradiance, with subtraction of the diffuse component), the result represents the ultimate validation of the new indoor methods 2, 3 and outdoor method 2.

It should also be noted that the level of reproducibility between Lab 1, 2, 3 and 6 is generally superior to the one observed between Lab 2, 4 and 5 using the same indoor method 2. However, it is also important to notice that, among these three laboratories, Lab 2 was the only one adopting a procedure for the subtraction of the diffuse component of irradiance indoors: this requirement is not present in Ed. 1.0 of IEC 61853-2, while the results of this interlaboratory comparison demonstrate its relevance.

4.3 The outlying results of Lab 4

As indicated in Table 2 and reminded above, Lab 4 did not adopt a correction procedure for the effect of stray light in the indoor method 2 like the one adopted by Lab 2. The observed hyper-cosine response measured by Lab 4, particularly pronounced in the Sanyo module (Figure 1a), may therefore arise from uncorrected straylight. This effect is likely caused by the secondary reflection by the module front glass incidence angles $\theta > 40^\circ$ to the walls of the darkroom and from there diffused back to the test sample, which may explain the scores $E_n > 1$ by Lab 4 at those angles for that module. The effect is only marginally present in the REC module, possibly due to the relatively lower I_{sc} of Sanyo, than REC values (see Table 1).

The secondary reflection effect is instead negligible in the Gintung module, due to its antiglare treatment: this may explain the satisfactory performance of Lab 4 on that sample (except at $\pm 80^\circ$, where the deviation is tight to the measurement uncertainty).

The results of Lab 4 stress the importance of the stray light correction in indoor measurements with methods 1 and 2, giving important feedback for the revision of IEC 61853-2. Correction for stray light is going to be included in a normative annexe of the new edition, based on the procedure described in [6] that has been successfully adopted by Lab 2.

4.4 The outlying results of Lab 5

The measurements of relative angular transmittance by Lab 5 showed a peculiar triangular shape at $\pm 40^\circ$ around normal incidence: Figure 4a-c show details of these findings (red crosses), compared to the assigned values (black continuous line). Conventional PV modules have usually symmetric relative angular transmittance and show cosine response in very good approximation between $\pm 20^\circ$, corresponding to a nearly zero slope in the $\tau_{rel}(\theta)$ curve around $\theta = 0$ in that interval and which is true for the three test samples

of this study.

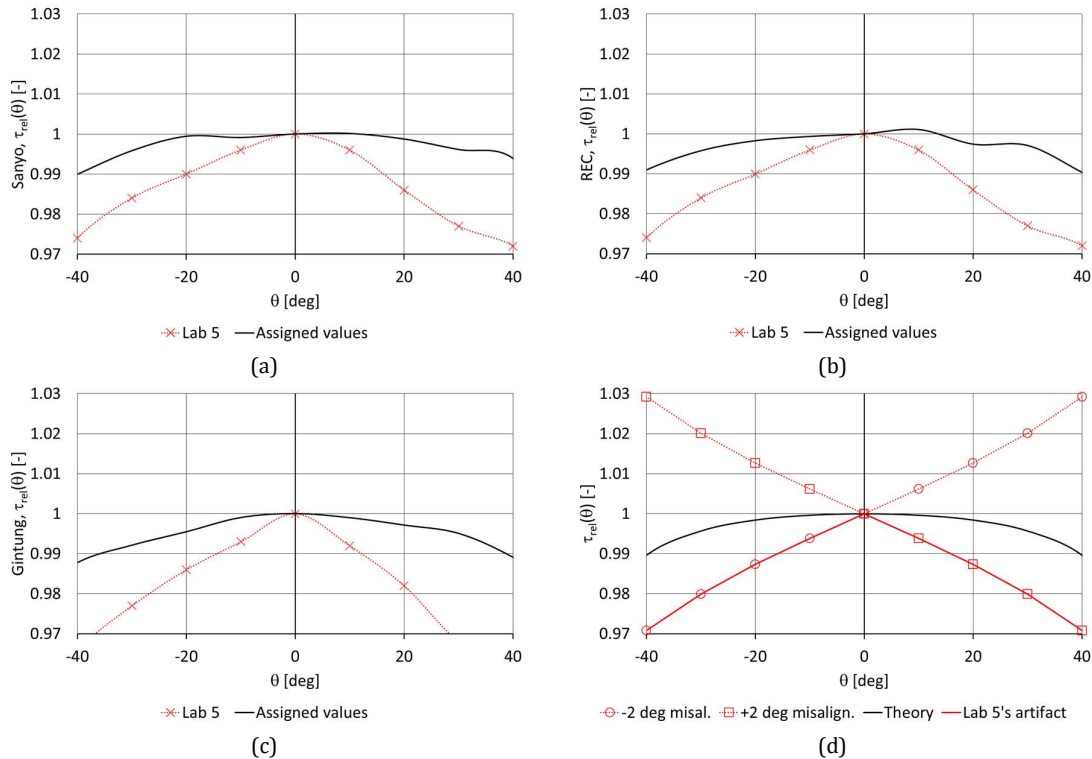


Figure 4: Observed triangular shape of relative angular transmittance measurements by Lab 5: (a) Sanyo; (b) REC; and (c) Gintung. (d) A theoretical comparison between a typically symmetric relative angular transmittance (continuous black line) and the corresponding tilted curves (in red) in which misalignments caused by offsets $\Delta\theta = -2^\circ$ (red circles) and $\Delta\theta = +2^\circ$ (red squares) were introduced: the continuous red line indicates the result of a possible measurement artifact consistent with the measurements reported by Lab 5.

In measurements of the incidence angle effect, uncorrected misalignments in the angular position at normal incidence result in measurement bias of hyper- or hypo-cosine response, as shown in Figure 4d. Here the circle and square dotted red lines show the effect of a misalignment $\Delta\theta = -2^\circ$ and $+2^\circ$, respectively, compared to the “theoretical”, unbiased and symmetric curve (continuous black line): the offset causes a measurement artifact of tilted $\tau_{rel}(\theta)$ curves. As reported by Lab 5, its equipment setting does not allow a complete rotation from -80 to $+80^\circ$, therefore the measurements were performed in 2 steps: first at positive angles; then the measurements at negative angles were obtained with the same verses of rotation, with the module rotated 180° . The findings of Figure 4a-c are therefore consistent with a systematic misalignment of the normal incidence condition by approximately $+2^\circ$, resulting in the triangular-shaped $\tau_{rel}(\theta)$ highlighted with the continuous red line of Figure 4d.

Uncertainty in misalignments of the order of $\pm 1^\circ$ may be common both with indoor and outdoor methods. In the indoor method, the uncertainty may arise because of imperfect alignment of the solar simulator lamp, or the non-collimated nature of the light source, or the inaccuracy in the point-like approximation: in fact, most simulators nowadays are multi-lamp and an alignment better than $\pm 1^\circ$ may not be technically feasible. However, correction for misalignment is possible, e.g. with optically alignment tools, or with quadratic interpolation of the measurement data around the nominal normal incidence.

The effect of misalignment in the results of Lab 5 was likely mitigated by the simultaneous effect of stray light, for which no correction procedure was adopted. That Lab 5 measurements were affected by stray light, could be inferred by the higher values of $\tau_{rel}(\theta)$ they reported on Sanyo and REC samples, with respect to the assigned values. This is a countertrend with the overall lower reported $\tau_{rel}(\theta)$ by Lab 5. Stray light effect (increasing of $\tau_{rel}(\theta)$) and $\Delta\theta = +2^\circ$ offset for both positive and negative angles (resulting in the triangular-shaped $\tau_{rel}(\theta)$) tend to compensate each other, with a result that the E_n score of Lab 5 is moderately satisfactory (a “false positive”). Gintung is again an exception: as observed with Lab 4 in the

previous section, the antiglare treatment of this module reduces significantly the effect of secondary reflections, hence in Lab 5 measurements the misalignment becomes a dominant bias, giving more questionable E_n scores.

4.5 The inadequacy of equation (1) fitting to the Gintung case

Figure 5 compares the assigned values for the measurements of $\tau_{\text{rel}}(\theta)$ of Gintung (black dots) with the interpolation based on equation (1) with the assigned value $a_r = 0.0757$ for that module (black line) and a set of other possible interpolations with a_r ranging from 0.025 to 0.2 (step 0.025, grey lines).

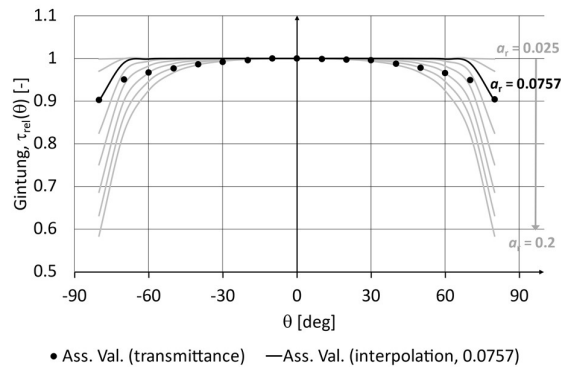


Figure 5: Assigned values for the relative angular transmittance measurements of Gintung (black dots), compared with the assigned values for the interpolation with $a_r = 0.0757$ (black line), and a set of interpolations from $a_r = 0.025$ to $a_r = 0.2$ (step 0.025, grey lines).

Although Figure 2 and Figure 3d showed a very good agreement for almost all laboratories in the evaluation of a_r for Gintung, the fitting of this interpolation with the assigned values of the measured relative angular transmittance of that module is highly questionable. In fact, the chart here highlights that the function in equation (1) is rather inadequate when trying to fit $\tau_{\text{rel}}(\theta)$ for a module with a special antiglare treatment like Gintung. Since the parameter a_r is used for energy rating purposes in the IEC 61853-3 [18], an action should be taken to suggest possible modifications of equation (1) in it to account for these cases: this is beyond the scopes of this exercise and represents an interesting indication for further works.

5 CONCLUSIONS

The incidence angle effect is showing growing interest among module manufacturers, developers and PV stakeholders as transmittance losses at wide angles may represent an important factor in the energy yield of PV installations. This work aimed at validating the new methods for measuring this effect that have been presented by various authors in recent years and are currently proposed for publication in the next edition of IEC 61853-2. Method validation was performed via interlaboratory comparison of the measurements of three commercial-size PV samples by six different testing laboratories with renowned expertise in the field.

The results of the exercise showed very good reproducibility on all samples of four over six participant laboratories, with some outliers from Lab 4 and 5. These have been discussed and highlighted the importance of two possible causes of measurement bias, e.g. the effect of stray light and angular misalignment. These effects can be corrected with accurate procedures that are going to be included as requirements in edition 2.0 of IEC 61853-2.

In terms of the interpolation parameter a_r , the exercise showed good overall reproducibility among all laboratories, with only few outliers, although this result may have been significantly affected by the large uncertainty with which this parameter is calculated. Furthermore, the inadequacy of equation (1) in IEC 61853-2 for modules with special antiglare treatment was highlighted, which may be a suggestion for improvement of the mathematical model behind it in further works.

ACKNOWLEDGMENTS

The authors would like to acknowledge SERIS for having provided the test samples. SERIS is a research institute at the National University of Singapore (NUS) and is supported by NUS, the National Research Foundation Singapore (NRF), the Energy Market Authority of Singapore (EMA), and the Singapore Economic Development Board (EDB).

REFERENCES

- [1] IEC 61853-2, "Photovoltaic (PV) module performance testing and energy rating – Part 2: Spectral responsivity, incidence angle and module operating temperature measurements" (2016).
- [2] IEC 60904-9, "Photovoltaic devices - Part 9: Classification of solar simulator characteristics" (2020).
- [3] N. Martin, and J. M. Ruiz, "Calculation of the PV modules angular losses under field conditions by means of an analytical model", *Solar Energy Materials & Solar Cells* **70**, 25-38 (2001).
- [4] N. Martin, and J. M. Ruiz, "Corrigendum to 'Calculation of the PV modules angular losses under field conditions by means of an analytical model'", *Solar Energy Materials & Solar Cells* **110**, 154, (2013).
- [5] W. Herrmann, M. Schweiger, L. Rimmelspacher, "Solar Simulator Measurement Procedures for Determination of the Angular Characteristic of PV Modules", *Proc. of the 29th European Photovoltaic Solar Energy Conference and Exhibition*, 2403-2406 (2014).
- [6] W. Herrmann, G. Bardizza, L. Rimmelspacher, M. H. Saw, M. Pravettoni, N. Riedel-Lyngskær, M. Babin, I. Kröger, "Test requirements for angular response measurement of encapsulated solar cell coupons", *Proc. of the 40th European Photovoltaic Solar Energy Conference and Exhibition* (2023).
- [7] H. Al Husna Binti Mohd Nasim, "Characterisation of spectral and angular effects on photovoltaic modules for energy rating", *PhD thesis*, Loughborough University (2018).
- [8] M. W. Amdemeskel, G. A. dos Reis Benatto, N. Riedel, B. Iandolo, R. S. Davidsen, O. Hansen, P. B. Poulsen, S. Thorsteinsson, A. Thorseth, C. Dam-Hansen, "Indoor measurement of angle resolved light absorption by antireflective glass in solar panels", *Proc. of the 34th European Photovoltaic Solar Energy Conference and Exhibition*, 1723-1726 (2017).
- [9] M. H. Saw, H. L. Soh, A. Ng, K. E. Birgersson, S. E. R. Tay, M. Pravettoni, "A spot-area method to evaluate the incidence angle modifier of photovoltaic devices — Part 1: Cells", *IEEE J. Photovolt.* **13**(2), 267-274 (2023).
- [10] M. Pravettoni, M. H. Saw, M. N. Bin Abdul Aziz, S. E. R. Tay, "A spot-area method to evaluate the incidence angle modifier of photovoltaic devices—Part 2: Modules", submitted to *IEEE J. Photovolt.*, under review.
- [11] F. Plag, I. Kröger, T. Fey, F. Witt, S. Winter, "Angular-dependent spectral responsivity—Traceable measurements on optical losses in PV devices", *Prog Photovolt Res Appl.* **26**, 565–578 (2018).
- [12] B. H. King, D. Riley, C. D. Robinson and L. Pratt, "Recent advancements in outdoor measurement techniques for angle of incidence effects," *Proc. of the IEEE Photovoltaic Specialist Conference (PVSC)*, New Orleans, LA, USA, (2015).
- [13] J. Coston, C. Robinson, B. King, J. Braid, D. Riley and J. S. Stein, "Effects of Solar Angle of Incidence on Intramodular Photovoltaic Irradiance Uniformity," *Proc. of the 48th IEEE Photovoltaic Specialists Conference (PVSC)*, 1499-1503 (2021).
- [14] S. Riechelmann, D. Friedrich, M. Müller, F. Schmaljohann, H. Sträter, S. Winter, "Primary Calibration of Solar Modules with Direct Sunlight", *Proc. of WCPEC-8*, 474-476 (2022).
- [15] A. van der Heide, A. Tuomiranta, M. Daniels, N. Capiot, M. Daenen, S. Wendlandt, L. Tous, "Accurate Measurement of the Angular Dependence of PV Module Performance Using a Dual Axis Solar Tracker", *Proc. of WCPEC-8*, 708-711 (2022).
- [16] ISO/IEC 17043, *Conformity assessment — General requirements for the competence of proficiency testing providers* (2023).
- [17] ISO 13528, *Statistical methods for use in proficiency testing by interlaboratory comparison* (2022).
- [18] IEC 61853-3, "Photovoltaic (PV) module performance testing and energy rating – Part 3: Energy rating of PV modules" (2018).